



HAB718 Spor Biyomekaniğinde Hareket Analizi



Serdar Arıtan

Hacettepe Üniversitesi
Spor Bilimleri Fakültesi
Biyomekanik Arařtırma Grubu

`serdar.aritan@hacettepe.edu.tr`



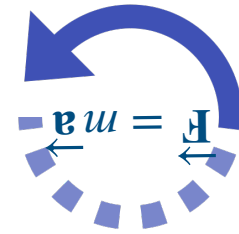
HAB718 Spor Biyomekaniğinde Hareket Analizi

#9

- Inverse Dynamics



HAB718 Spor Biyomekaniğinde Hareket Analizi



Inverse Dynamics

8

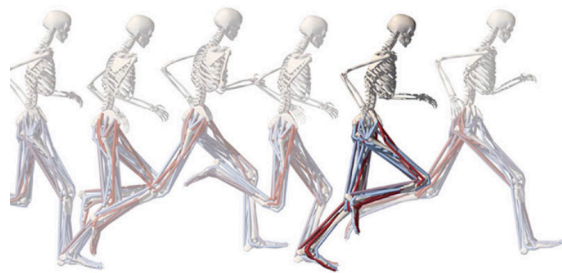
Inverse Dynamics

To every action there is always opposed an equal reaction.

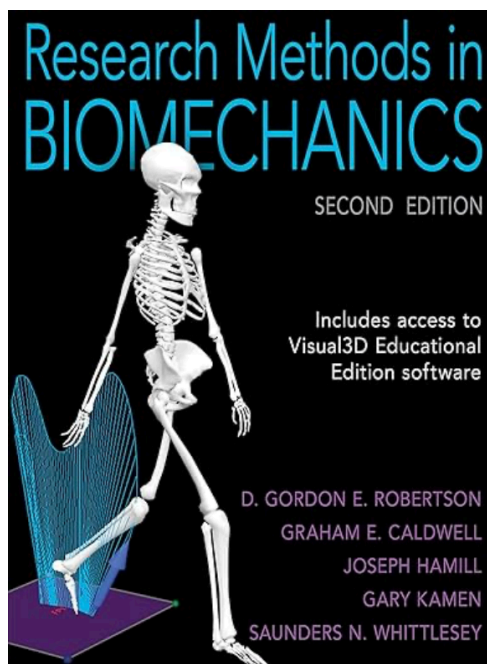
—Sir Isaac Newton

Biomechanics OF Movement

THE SCIENCE OF SPORTS, ROBOTICS, AND REHABILITATION



Thomas K. Uchida AND Scott L. Delp
ILLUSTRATIONS BY David Delp



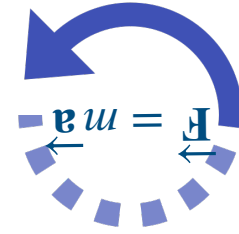
Chapter 7

Three-Dimensional Kinetics

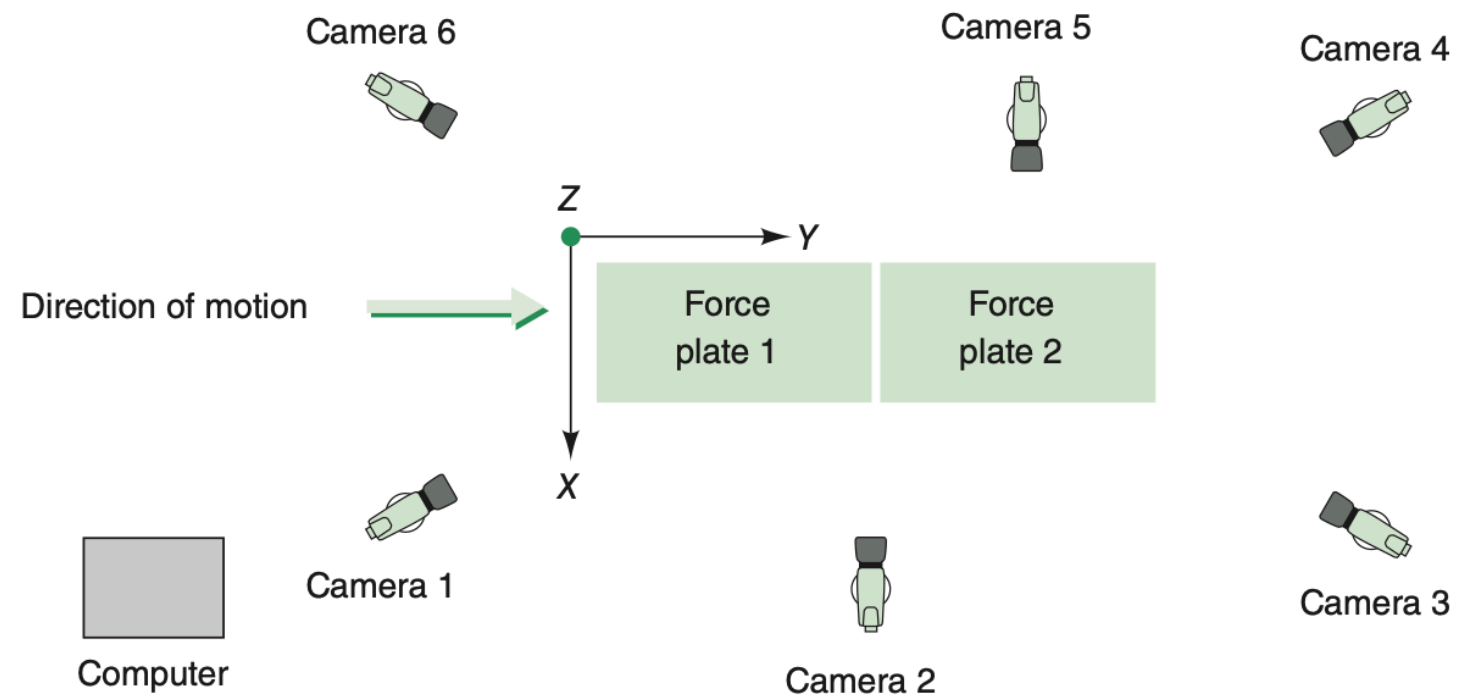
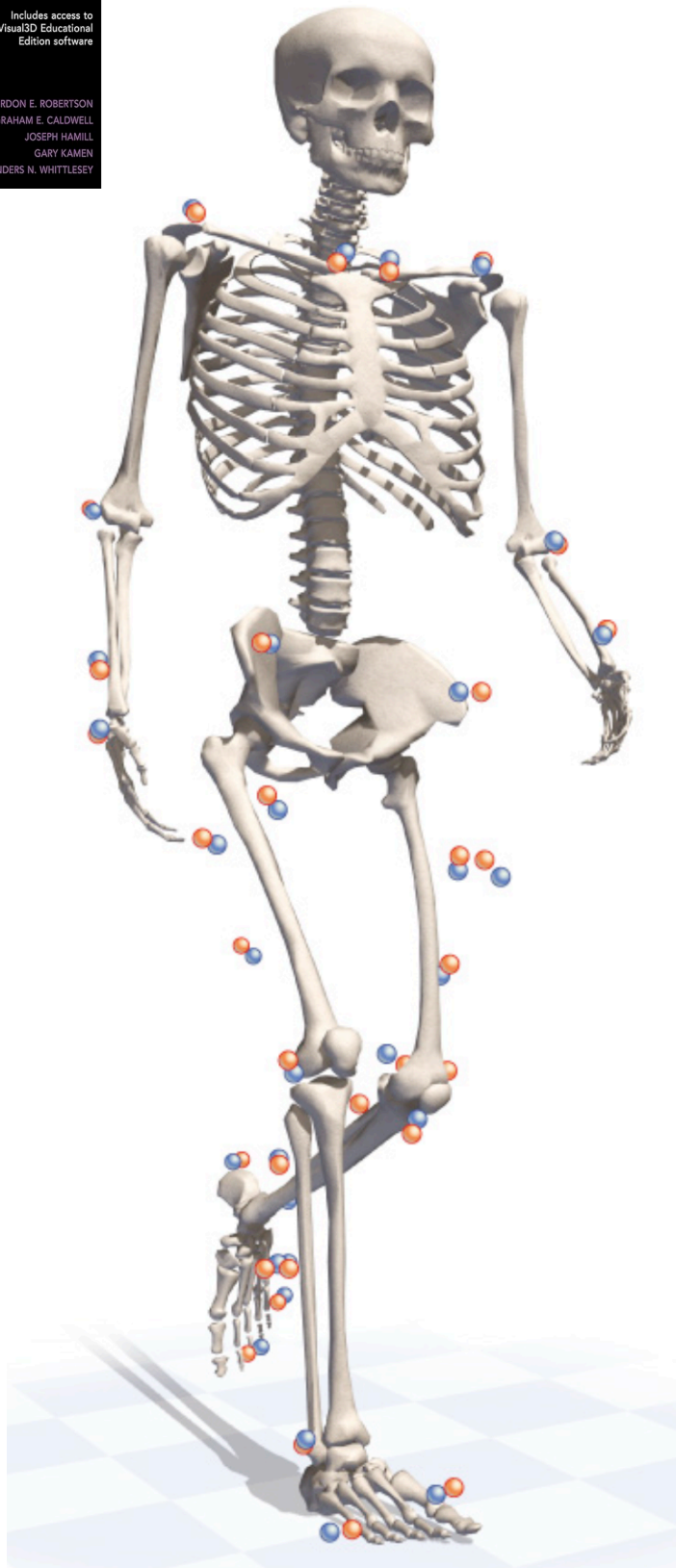
W. Scott Selbie, Joseph Hamill, and Thomas M. Kepple



HAB718 Spor Biyomekaniğinde Hareket Analizi

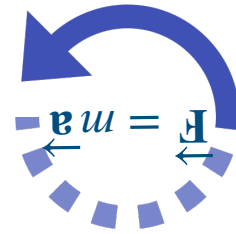


Inverse Dynamics



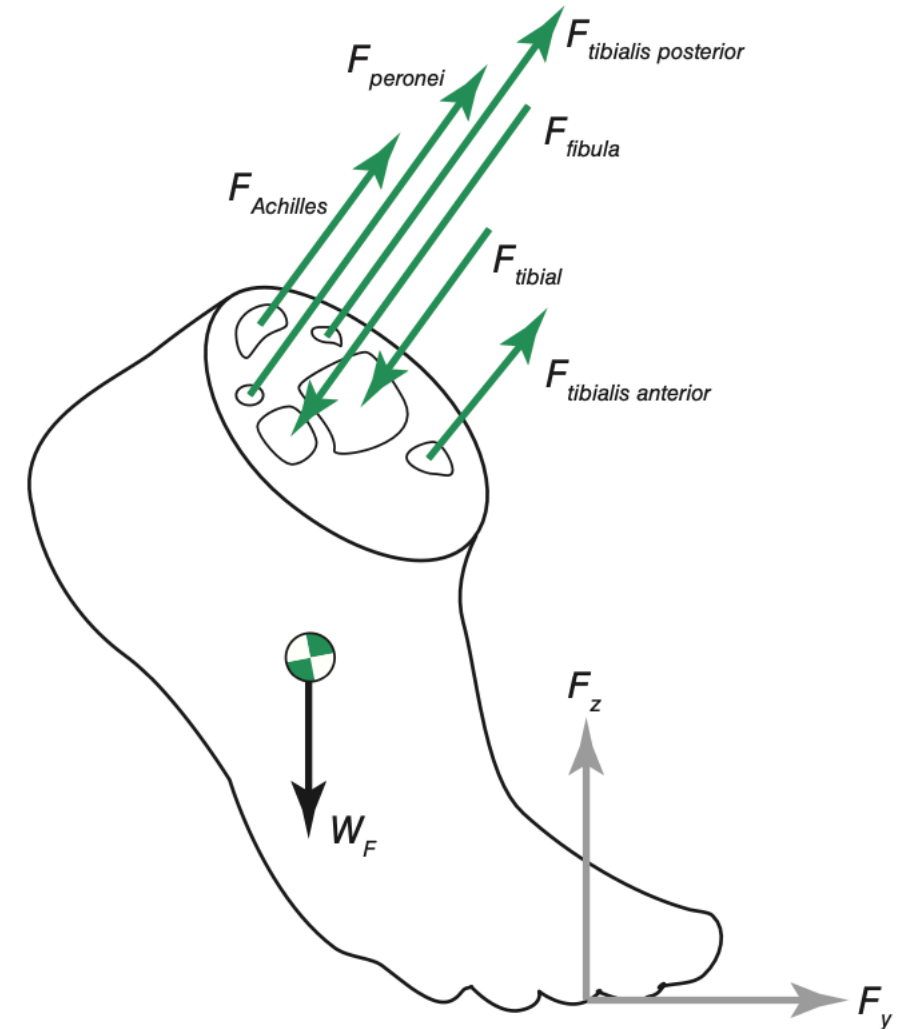


HAB718 Spor Biyomekaniğinde Hareket Analizi



Inverse Dynamics

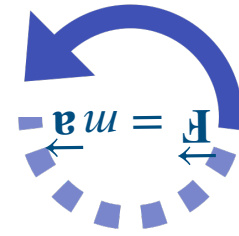
The joint reaction force computed at the joint is independent of this compressive load, and the net compressive load (**joint reaction force plus muscle compressive load**) cannot be computed from the methods of this chapter.



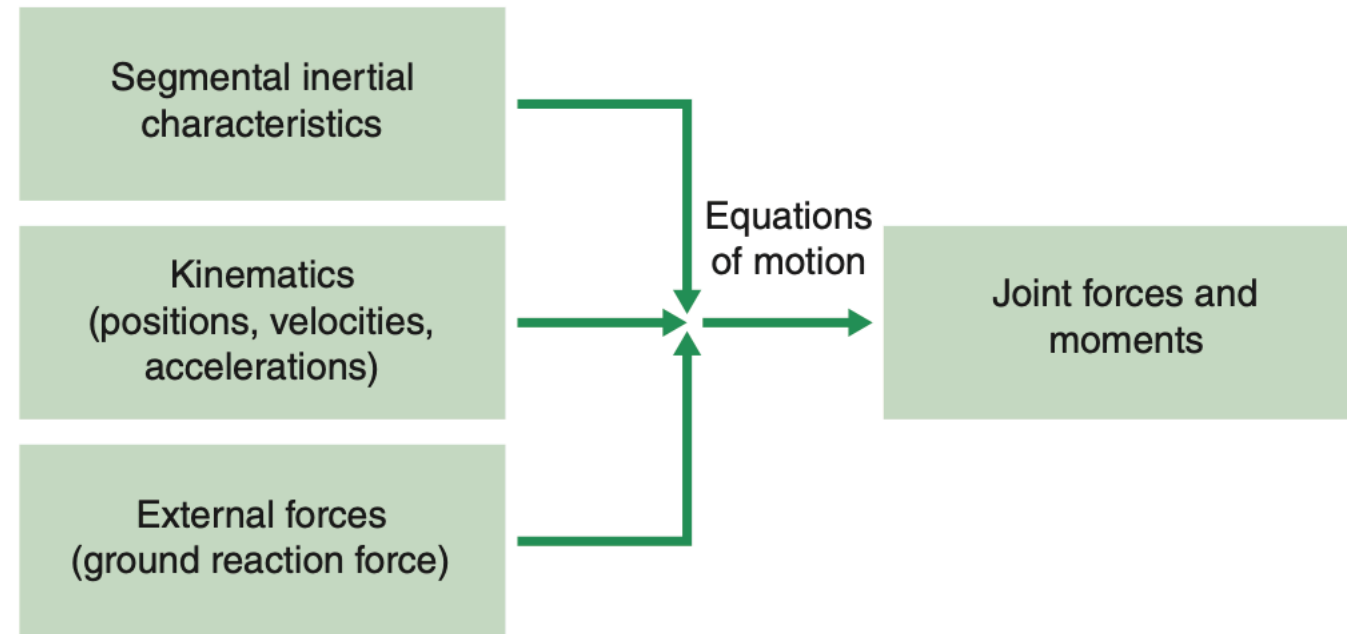
▲ **Figure 7.2** A free-body diagram of the foot with all external forces identified.

Reprinted from *Human Movement Science*, Vol. 15, C.L. Vaughan, "Are joint moments the holy grail of human gait analysis?" pgs. 423-443, copyright 1996, with permission of Elsevier.

HAB718 Spor Biyomekaniğinde Hareket Analizi



Inverse Dynamics



▲ **Figure 7.4** Flowchart of the inverse dynamics approach.

1. Define the segment local coordinate systems (LCS) (see chapter 2).
2. Estimate the pose of the model from recorded motion-capture data (see chapter 2).
3. Scale the segment anthropometry to the subject and identify the segment inertial characteristics (also chapter 4).
4. Compute kinematics (e.g., angular velocities and accelerations) from the pose estimates (see chapter 2).
5. Record and represent external forces acting on the body.
6. Compute the joint reaction forces, net joint moments, and joint powers.

HAB718 Spor Biyomekaniğinde Hareket Analizi

Inverse Dynamics



The first devices for measuring foot–ground contact forces were designed in the **late 1800s** by Étienne-Jules Marey and his student Gaston Carlet. By embedding pressure transducers into the sole of a shoe, Marey and Carlet were able to estimate the forces exerted between the foot and the ground during gait.

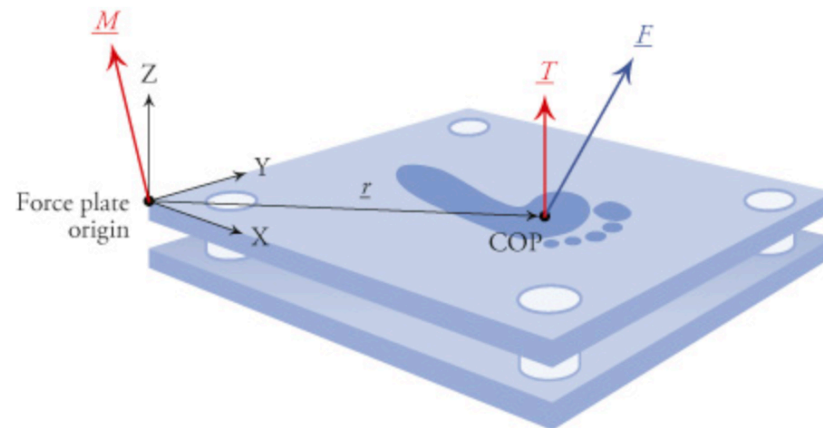


Figure 8.2 A force plate measures the forces and moments applied between the ground and the subject, collectively referred to as ground reaction forces. The center of pressure (COP) and the “free moment” (\underline{T}) can be computed from the resultant force (\underline{F}) and total moment (\underline{M}).

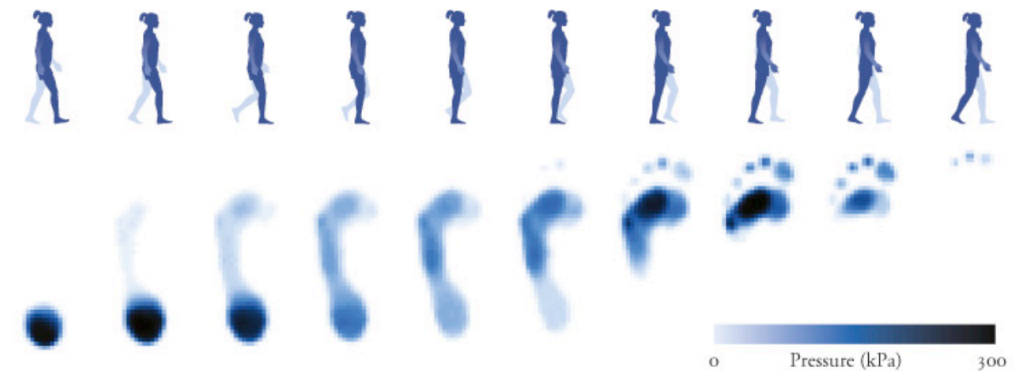
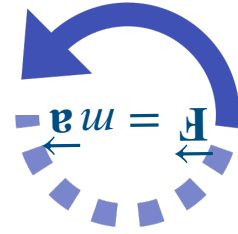


Figure 8.3 Pressure distributed over the foot during walking. Adapted from Pataky et al. (2012).

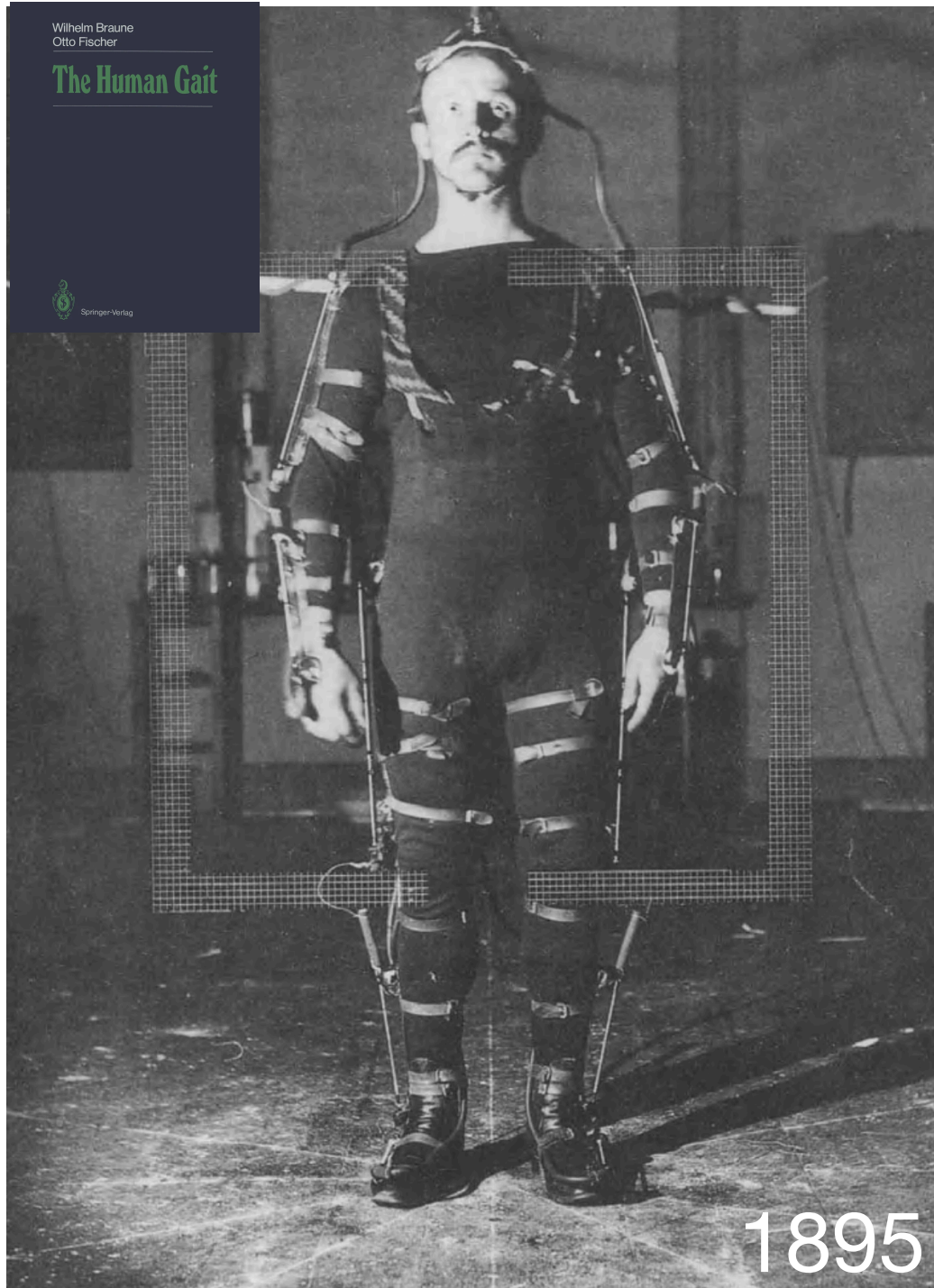
$$\underline{M} = \underline{r} \times \underline{F} + \underline{T} \quad (8.1)$$



HAB718 Spor Biyomekaniğinde Hareket Analizi



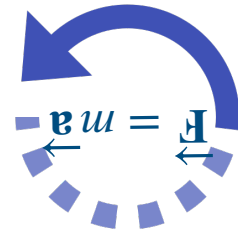
Inverse Dynamics



In order to analyse walking we modified the method which we had used to measure movement of the knee: **we illuminated different parts of the human body by Geissler tubes rather than electric sparks.** These tubes were filled with rarefied nitrogen since, when incandescent, this gas emits many chemically active rays. In order to record the successive positions of the human body in walking without taking into account the contingent deformations of the hand and foot, **it would have been sufficient to attach small tubes to all the big joints.** However, we decided to use long, thin, straight tubes, so as to provide a better overall view of the changes in the position of the body and a more reliable determination of the successive phases of the different curves of displacement. The tubes were attached to, e. g. the upper arm and thigh (between the two adjacent joints), the forearm, lower leg and foot (from one of the two joints to beyond the middle of the limb). The experimental subject wore a black jersey suit (Fig. 5), similar to the one used by Marey. The suit provided a dark background for the tubes and permitted better attachment of the tubes to the body.



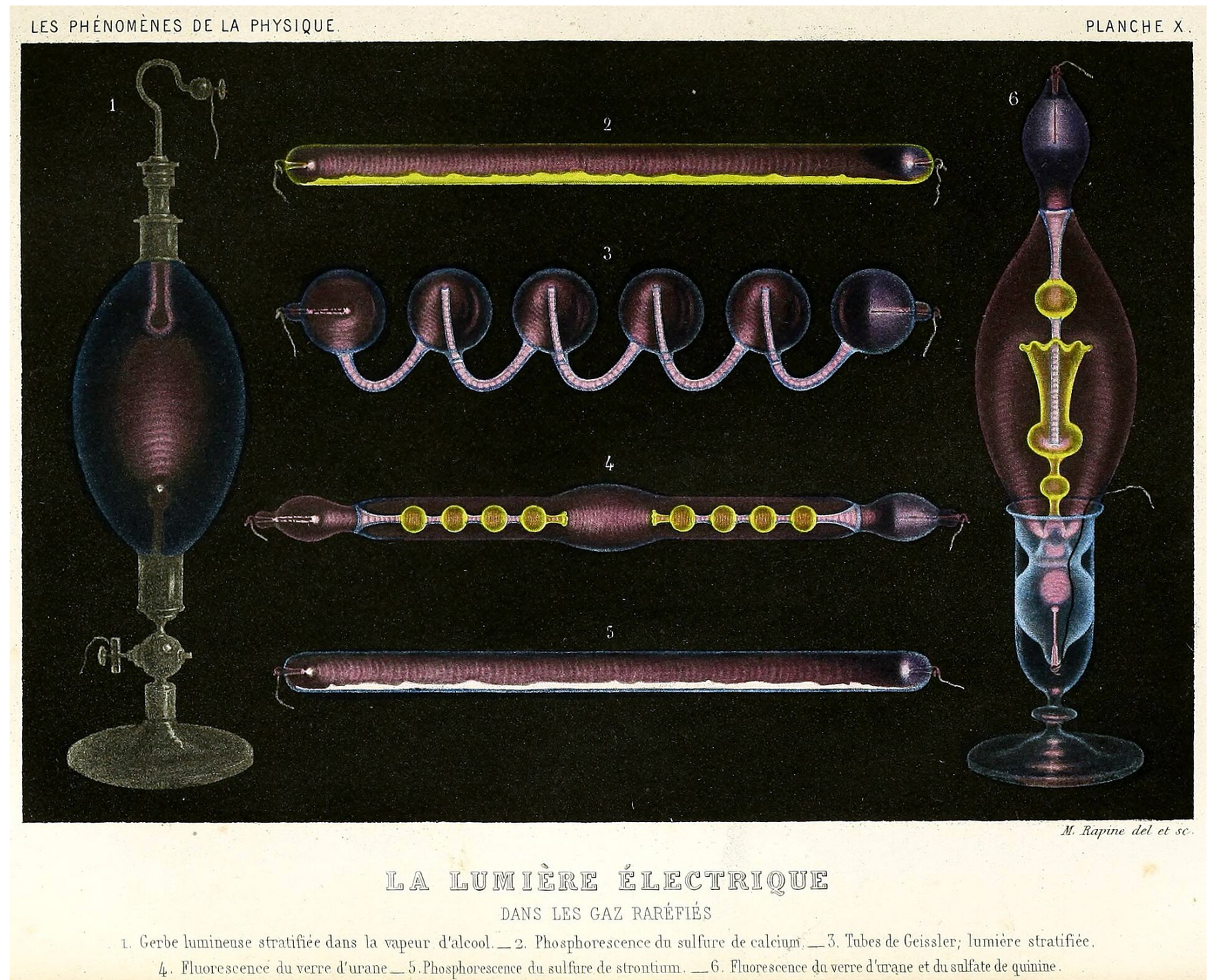
HAB718 Spor Biyomekaniğinde Hareket Analizi



Inverse Dynamics

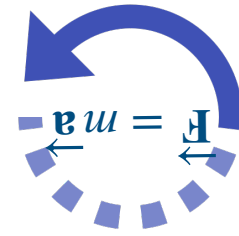


Heinrich Geissler
(1814 - 1879)

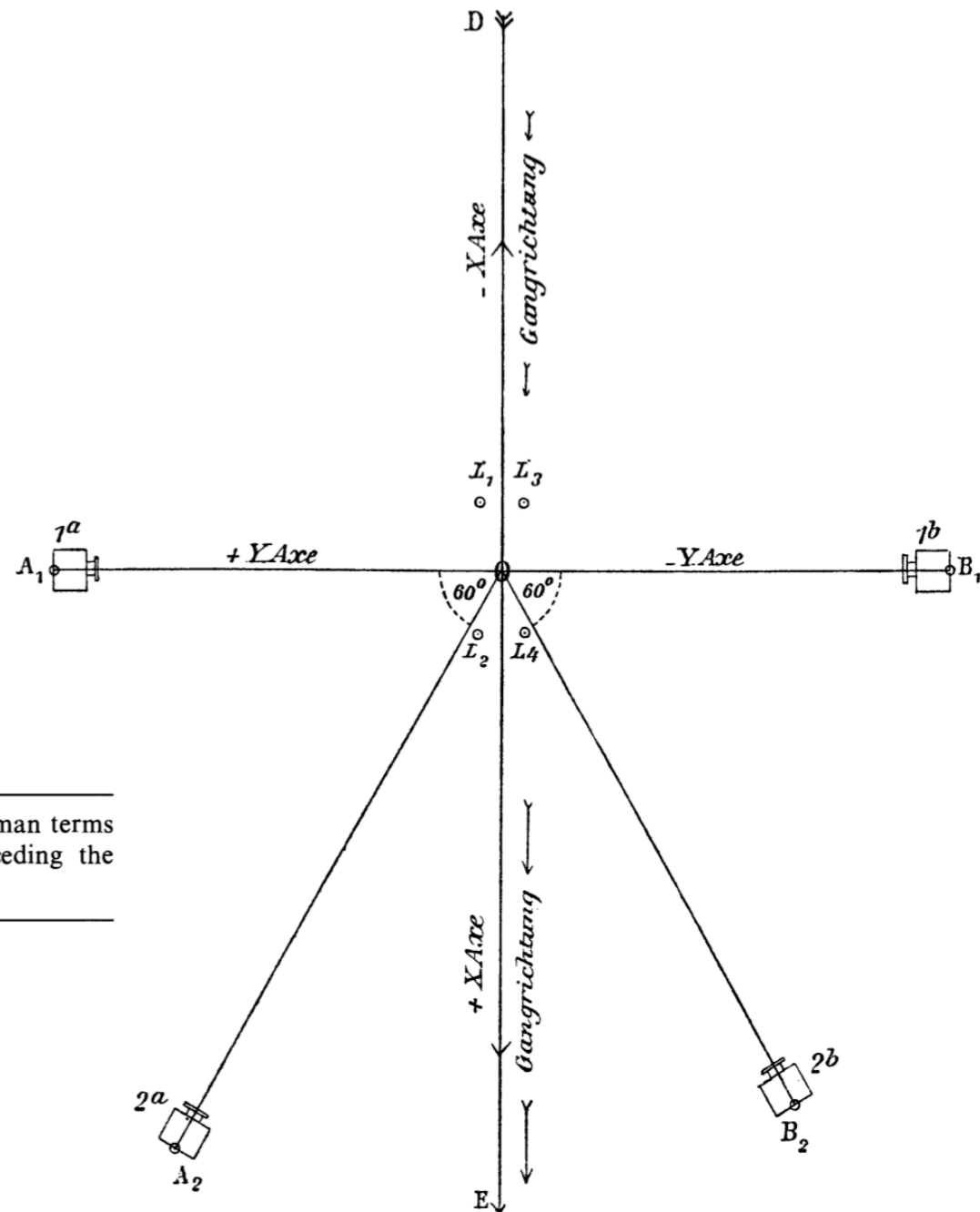
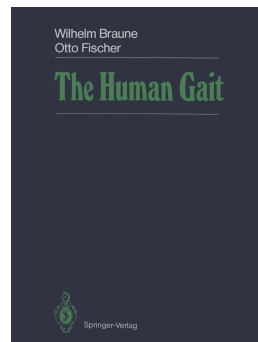


Drawing of Geissler tubes illuminated by their own light, from 1868 French physics book, showing some of the many decorative shapes and colors

HAB718 Spor Biyomekaniğinde Hareket Analizi



Inverse Dynamics



Note: For English translation of the German terms please turn to overleaf page preceding the Name and Subject Index

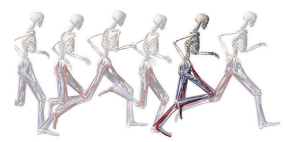
Fig. 6. Calculation of the tridimensional rectangular co-ordinates x , y , z from the projections of an object on the planes at right angles to the optical axes of cameras



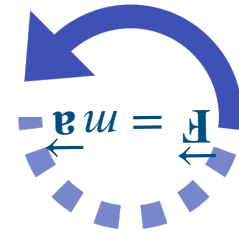
HAB718 Spor Biyomekaniğinde Hareket Analizi

Biomechanics
OF Movement

THE SCIENCE OF SPORTS, ROBOTICS, AND REHABILITATION



Thomas K. Uchida AND Scott L. Delp
ILLUSTRATIONS BY David Delp



Inverse Dynamics

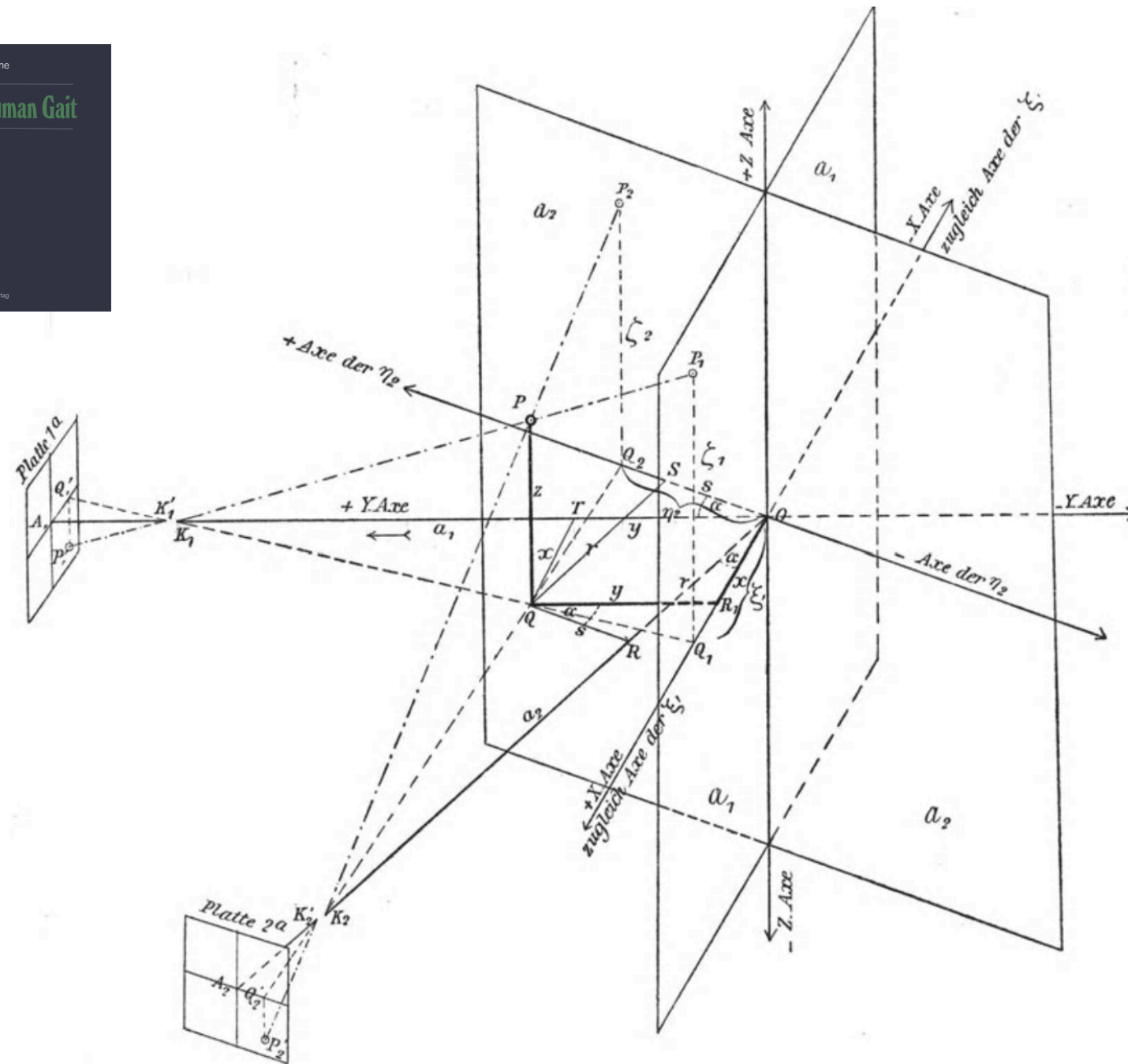
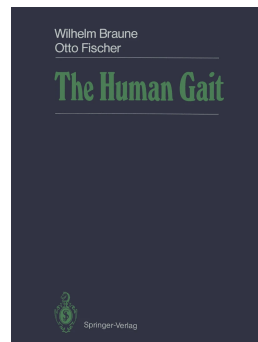
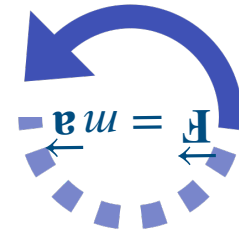


Fig. 11. Determination of the co-ordinates of a point P from the projections of P on two planes a_1 and a_2 as seen from cameras 1^a and 2^a

HAB718 Spor Biyomekaniğinde Hareket Analizi



Inverse Dynamics

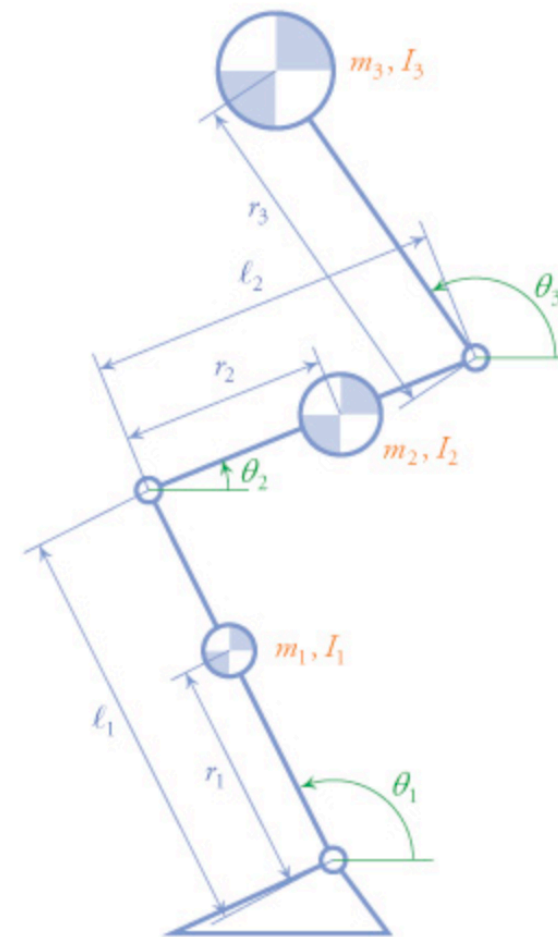


Figure 8.4 Experimental setup (left) and approximate sagittal-plane model (right) for studying a squat. An inverse dynamic analysis computes the net forces and moments at each joint from the mass, inertia, geometry, and kinematics (positions, velocities, and accelerations) of each body segment (as well as external forces, when available).

HAB718 Spor Biyomekaniğinde Hareket Analizi

Inverse Dynamics

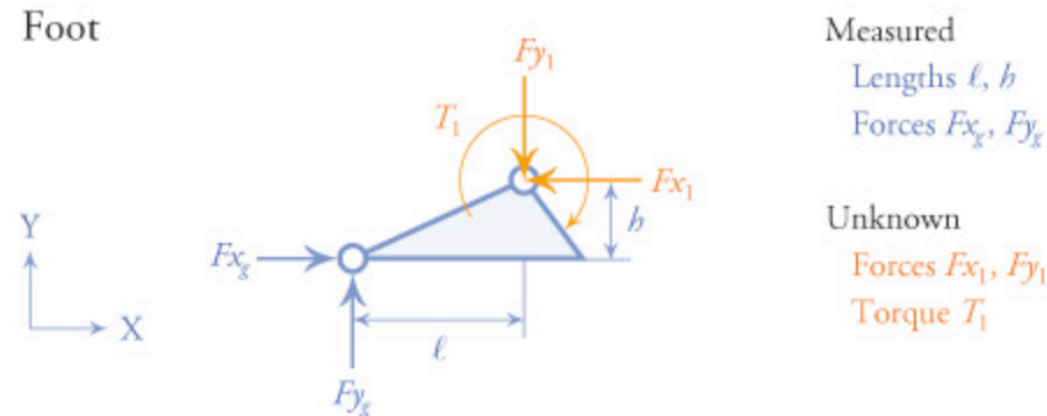


Figure 8.5 Free-body diagram for the foot segment of the model shown in Figure 8.4.

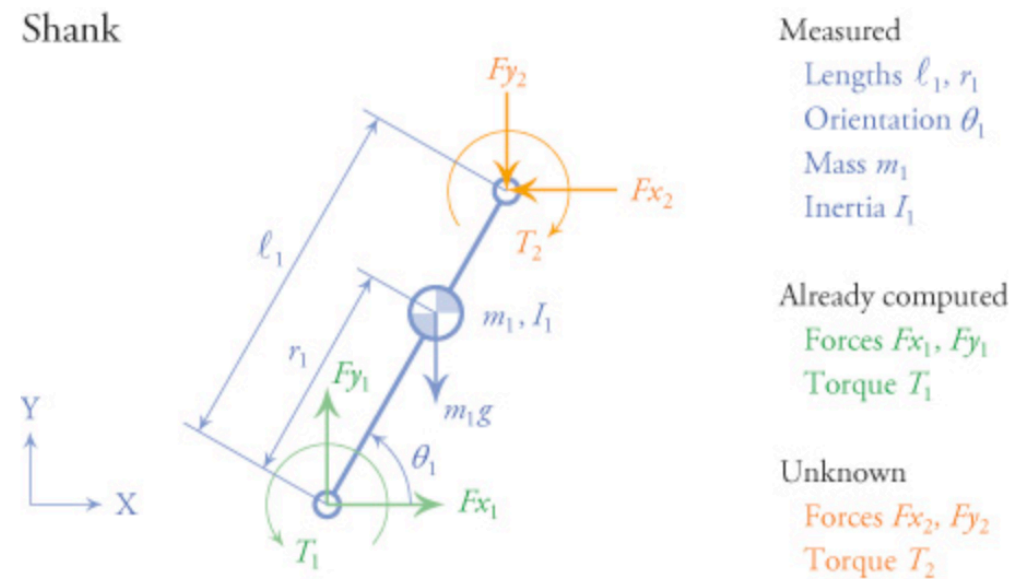
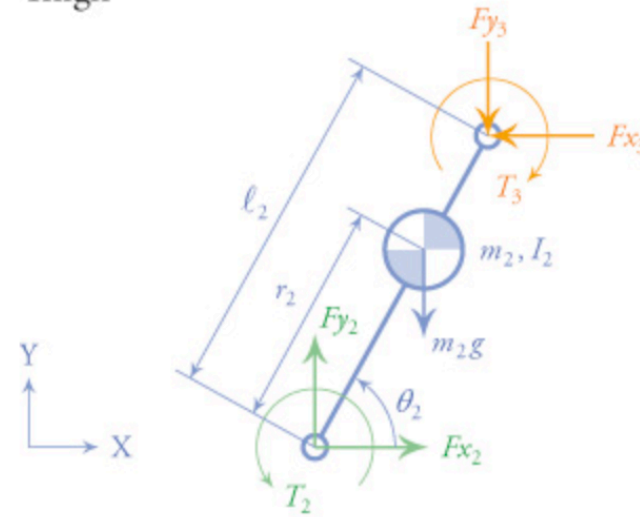


Figure 8.6 Free-body diagram for the shank segment of the model shown in Figure 8.4. The pose of the body segment in a free-body diagram need not match its pose during the activity being studied. Although irrelevant mathematically, we draw the shank segment in this convenient canonical pose, where θ_1 is between 0 and 90 degrees.

HAB718 Spor Biyomekaniğinde Hareket Analizi

Inverse Dynamics

Thigh



Measured

Lengths ℓ_2, r_2
Orientation θ_2
Mass m_2
Inertia I_2

Already computed

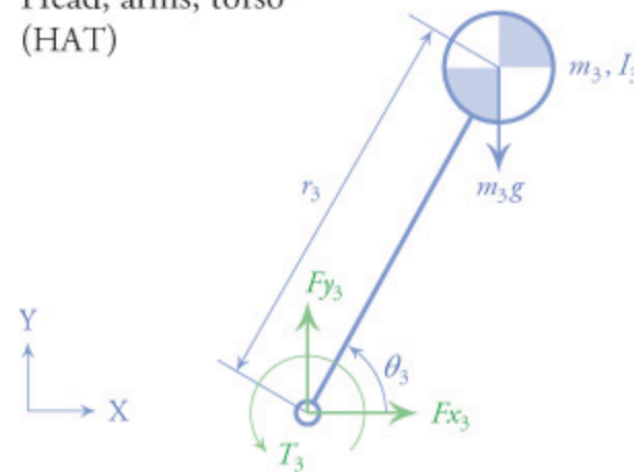
Forces F_{x2}, F_{y2}
Torque T_2

Unknown

Forces F_{x3}, F_{y3}
Torque T_3

Figure 8.7 Free-body diagram for the thigh segment of the model shown in Figure 8.4.

Head, arms, torso
(HAT)



Measured

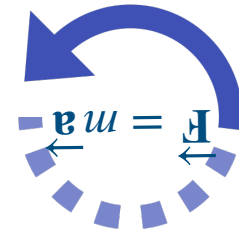
Length r_3
Orientation θ_3
Mass m_3
Inertia I_3

Already computed

Forces F_{x3}, F_{y3}
Torque T_3

Figure 8.8 Free-body diagram for the head, arms, and torso (HAT) of the model shown in Figure 8.4.

HAB718 Spor Biyomekaniğinde Hareket Analizi



Inverse Dynamics

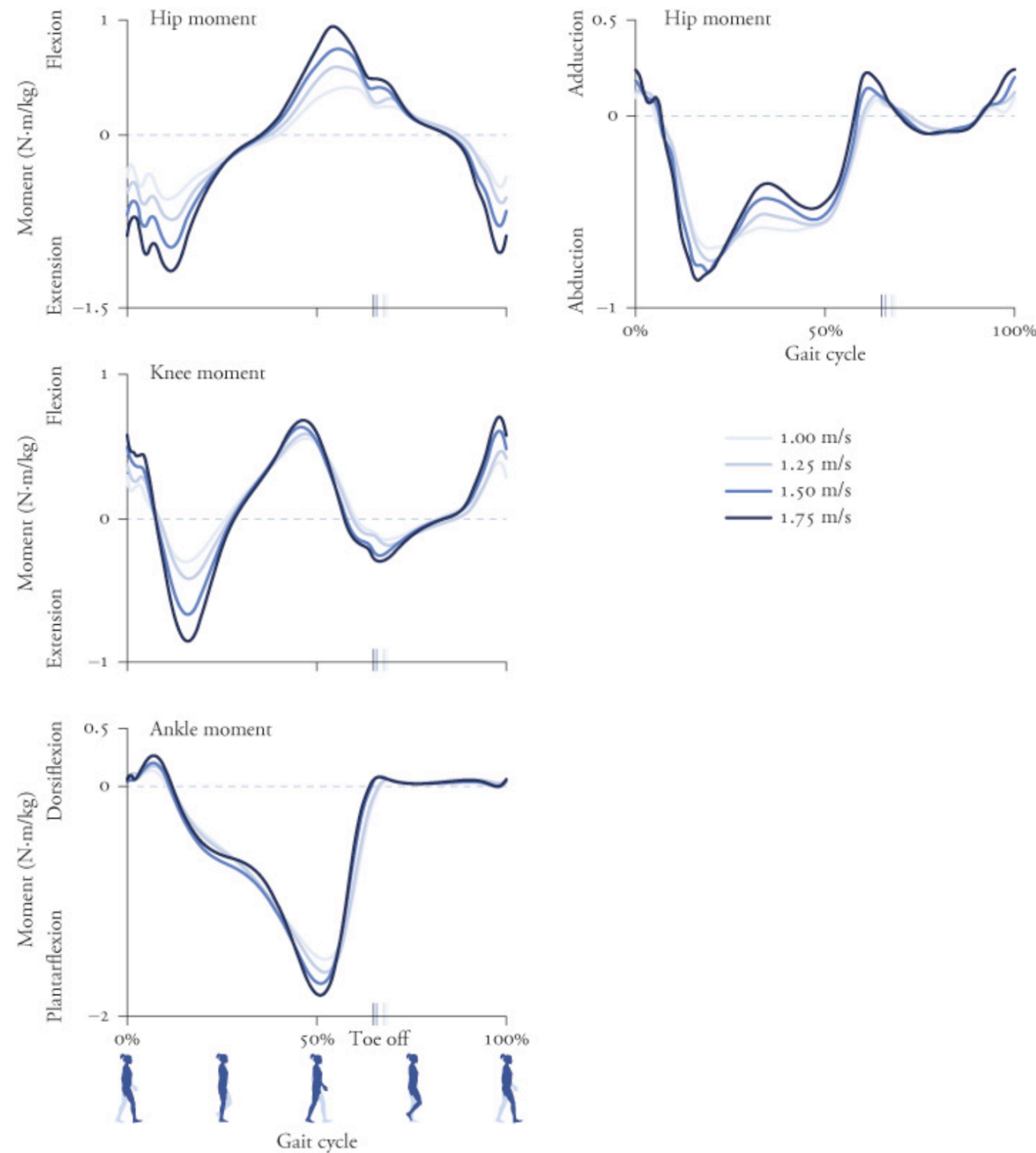
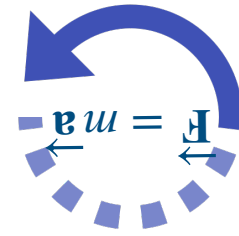


Figure 8.9 Representative joint moments over the gait cycle when walking at several speeds. Normalized by body mass and averaged over 10 subjects. Vertical lines on the horizontal axis indicate toe off at each speed. Data from Arnold et al. (2013).

HAB718 Spor Biyomekaniğinde Hareket Analizi



Inverse Dynamics

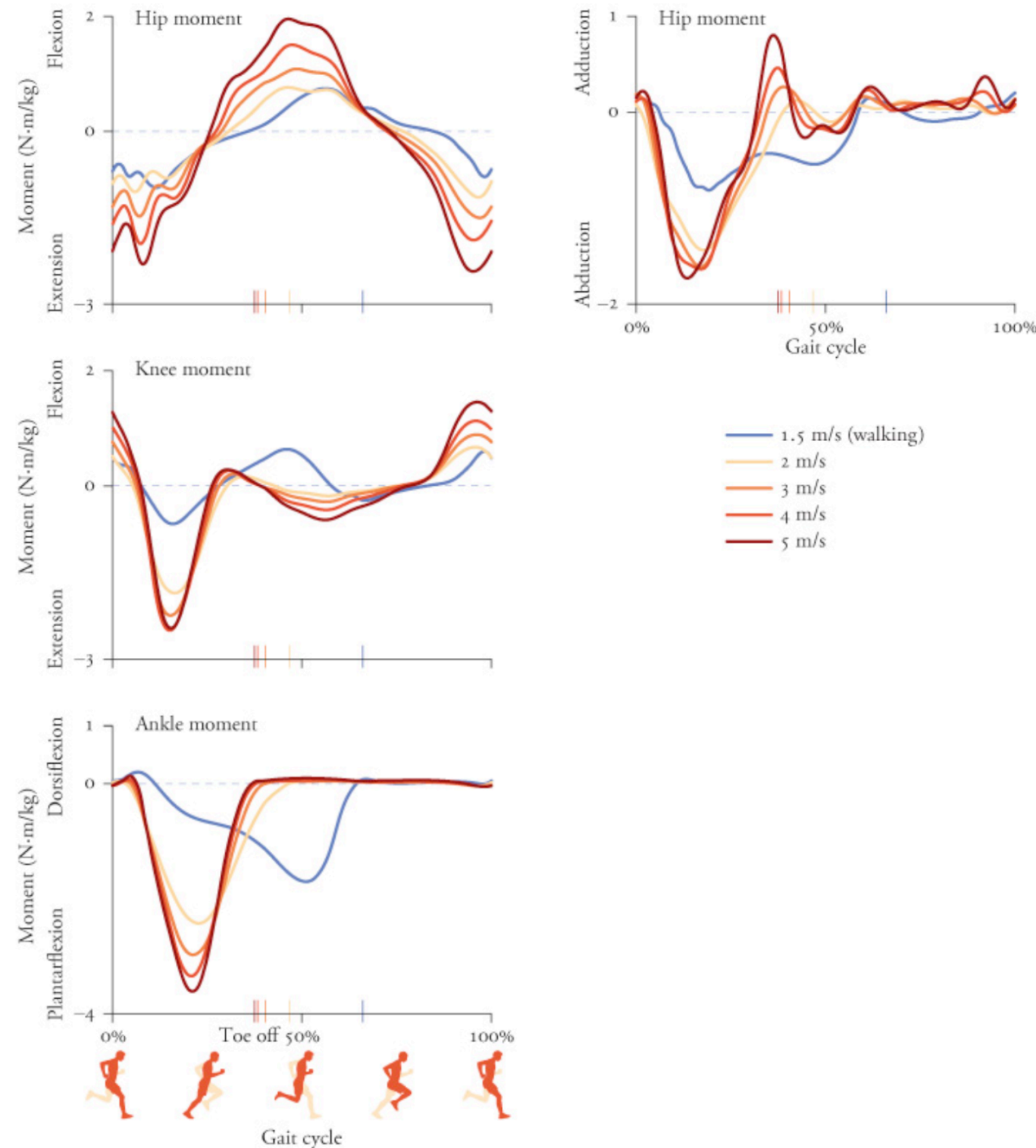
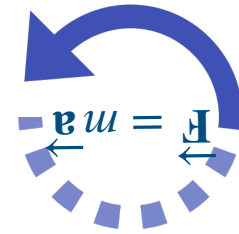


Figure 8.10 Representative joint moments over the gait cycle when running at several speeds (walking at 1.5 m/s from Figure 8.9 is shown for reference). Normalized by body mass and averaged over 10 subjects. Vertical lines on the horizontal axis indicate toe off at each speed. Data from Hamner and Delp (2013).

HAB718 Spor Biyomekaniğinde Hareket Analizi

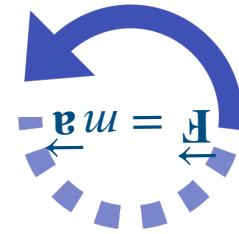


Inverse Dynamics

The major drawback of inverse dynamics analysis using **motion-capture data** is the compilation of errors from all the measurements and calculations required to derive joint torque estimates. These errors arise from a variety of sources, including experimental and systemic errors, and are worth an exhaustive description.

First, the measurement of marker position data in real-time has associated errors from noise and calibration inaccuracies. When joint centers are approximated by marker locations a difference invariably exists between the modeled center of rotation and the anatomical joint center. The repeatability of marker placement on the body contributes to this issue. Even if the markers were able to be placed with perfect accuracy and exact repeatability and precisely tracked, the soft tissues of the limbs allow the marker to move relative to the bone. Error in the marker position data also compounds when numerically differentiating the discrete data points to obtain segment velocities and again when calculating accelerations.

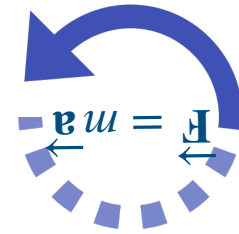
HAB718 Spor Biyomekaniğinde Hareket Analizi



Inverse Dynamics

All of these errors compound when moving along the chain of segments, getting progressively worse at each step. Because each segment solution depends on the reaction forces from the previous segment, any errors in the calculated values for one segment will propagate to the adjacent segments. Thus, the accuracy of forces and torques calculated on the first segment has a profound effect on the reliability of the calculated values further up the model. Since the forces and torques are calculated directly from the second derivative of position data from a video motion capture system, any noise in the position measurement increases non-linearly in the calculation of velocity, and again for acceleration. **Kuo (1998)** proposed an alternative method for inverse dynamics which solves all of the equations simultaneously in a least squares sense to find the joint torques that best satisfy the equations. Kuo demonstrated a 30% reduction in error in calculated joint torques compared to a conventional analysis, with both solutions being compared to a forward simulation. **Van den Bogert et al. (2008)** proposed an alternative method also using a least squares solution, which expanded on Kuo's work to a 3-dimensional system and analysis of partial ground reaction data. They compared the error between the conventional and alternative methods on measured data, and compared noise to estimated noise derived from a Monte Carlo simulation.

HAB718 Spor Biyomekaniğinde Hareket Analizi



Inverse Dynamics

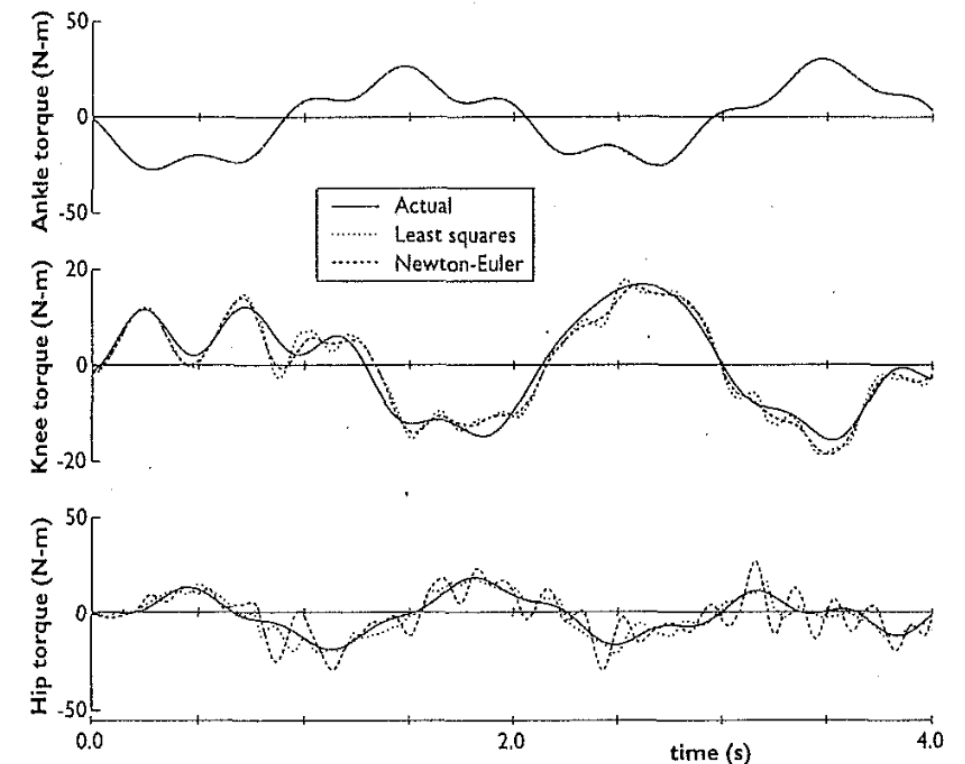
A Least-Squares Estimation Approach to Improving the Precision of Inverse Dynamics Computations

A. D. Kuo

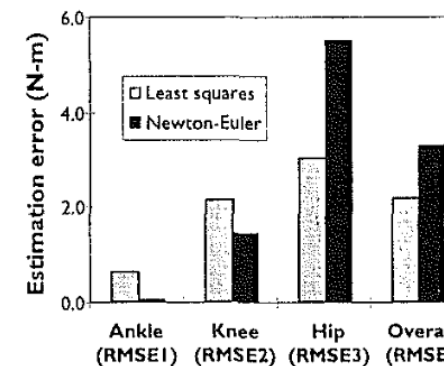
Department of Mechanical Engineering &
Applied Mechanics,
University of Michigan,
Ann Arbor, MI 48109

A least-squares approach to computing inverse dynamics is proposed. The method utilizes equations of motion for a multi-segment body, incorporating terms for ground reaction forces and torques. The resulting system is overdetermined at each point in time, because kinematic and force measurements outnumber unknown torques, and may be solved using weighted least squares to yield estimates of the joint torques and joint angular accelerations that best match measured data. An error analysis makes it possible to predict error magnitudes for both conventional and least-squares methods. A modification of the method also makes it possible to reject constant biases such as those arising from misalignment of force plate and kinematic measurement reference frames. A benchmark case is presented, which demonstrates reductions in joint torque errors on the order of 30 percent compared to the conventional Newton-Euler method, for a wide range of noise levels on measured data. The advantages over the Newton-Euler method include making best use of all available measurements, ability to function when less than a full complement of ground reaction forces is measured, suppression of residual torques acting on the top-most body segment, and the rejection of constant biases in data.

a. Joint torque estimates



c. Torque error



d. Acceleration error

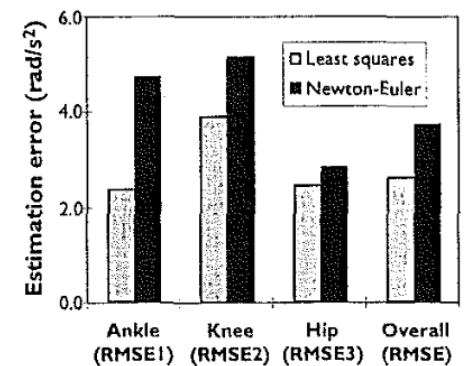
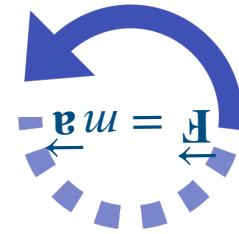


Fig. 3 Comparison of results from benchmark test of Newton-Euler and least-squares methods. Least-squares method substantially improves estimates for joints distal to force plate, resulting in lower overall error. (a) Joint torque estimates over time, versus actual torques at ankle, knee, and hip. (b) Joint torque estimation error, averaged over time, for each joint and overall error (RMSE). (c) Joint angular acceleration estimation errors, averaged over time, are reduced using least-squares method for all joints.

HAB718 Spor Biyomekaniğinde Hareket Analizi



Inverse Dynamics

Computer Methods in Biomechanics and Biomedical Engineering,
Vol. 11, No. 1, February 2008, 3–9



A weighted least squares method for inverse dynamic analysis*

ANTONIE J. VAN DEN BOGERT^{†‡*} and ANNE SU^{¶§}

[†]Department of Biomedical Engineering, Cleveland Clinic Foundation, Cleveland, OH, USA

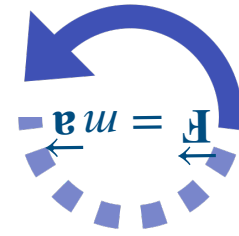
[‡]Orthopaedic Research Center, Cleveland Clinic Foundation, Cleveland, OH, USA

[¶]Department of Anthropology, State University of New York, Stony Brook, NY, USA

Internal forces in the human body can be estimated from measured movements and external forces using inverse dynamic analysis. Here we present a general method of analysis which makes optimal use of all available data, and allows the use of inverse dynamic analysis in cases where external force data is incomplete. The method was evaluated for the analysis of running on a partially instrumented treadmill. It was found that results correlate well with those of a conventional analysis where all external forces are known.

Keywords: Inverse dynamics; Gait analysis; Multibody dynamics; Ground reaction force

HAB718 Spor Biyomekaniğinde Hareket Analizi



Inverse Dynamics

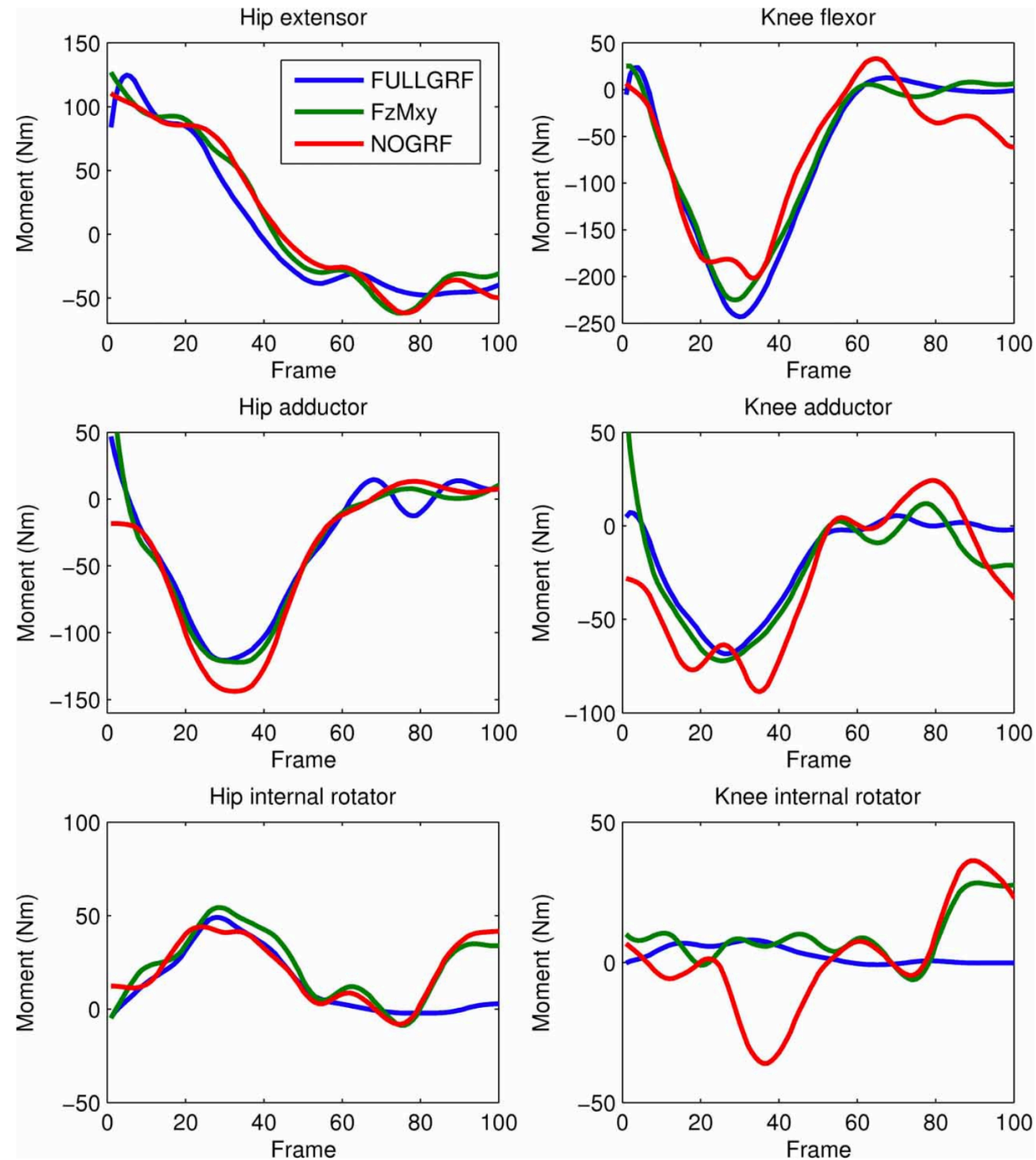
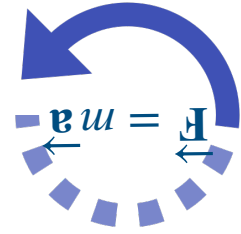


Figure 2. Three dimensional joint moments at hip and knee during a representative running trial, obtained with each of the three inverse dynamics methods. Frame rate is 240 Hz and frame 1 represents heel strike.



HAB718 Spor Biyomekaniğinde Hareket Analizi

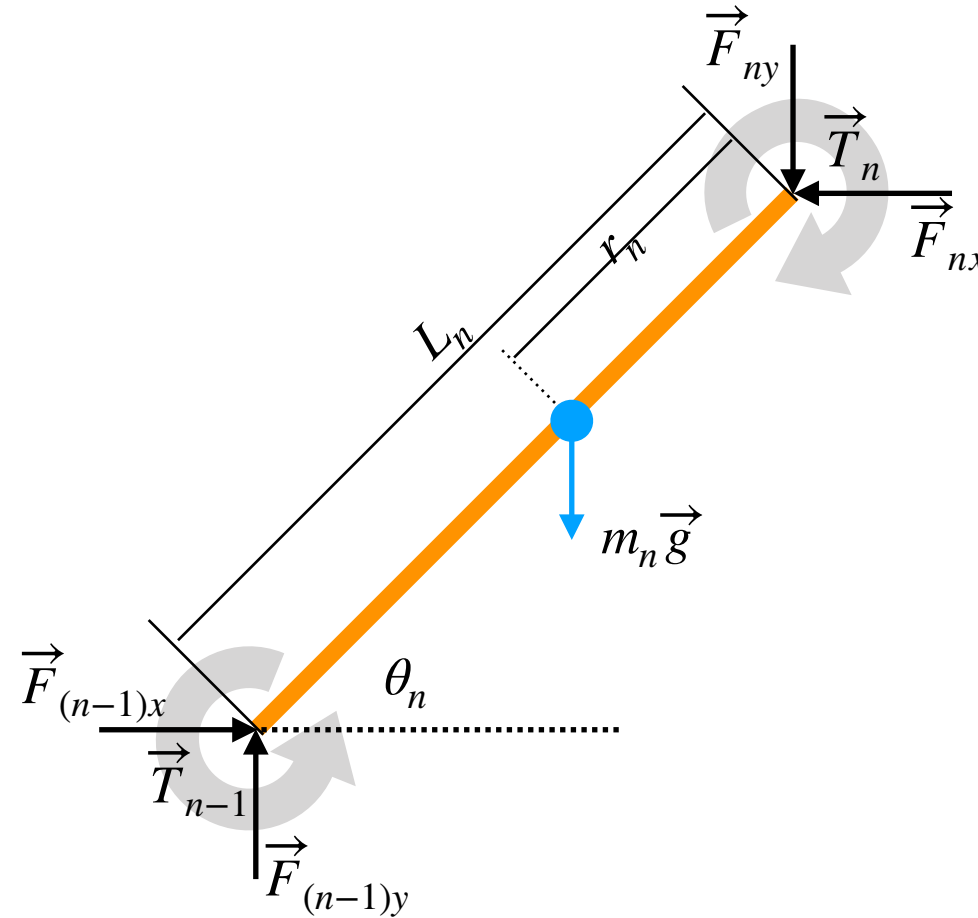


Inverse Dynamics

$$\sum \vec{F}_{nx} = m_n \vec{a}_{nx}$$

$$\sum \vec{F}_{ny} = m_n \vec{a}_{ny}$$

$$\sum \vec{T}_n = I_n \vec{\alpha}_n$$



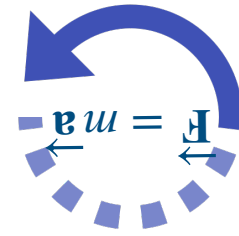
$$-m \vec{a}_{nx} + \vec{F}_{(n-1)x} - \vec{F}_{nx} = 0$$

$$-m \vec{a}_{ny} + \vec{F}_{(n-1)y} - \vec{F}_{ny} - m \vec{g} = 0$$

$$-I_n \vec{\alpha}_n + \vec{T}_{n-1} - \vec{T}_n + \vec{F}_{(n-1)x}(L_n - r_n)\sin\theta_n - \vec{F}_{(n-1)y}(L_n - r_n)\cos\theta_n + \vec{F}_{nx}r_n\sin\theta_n - \vec{F}_{ny}r_n\cos\theta_n = 0$$



HAB718 Spor Biyomekaniğinde Hareket Analizi



Inverse Dynamics

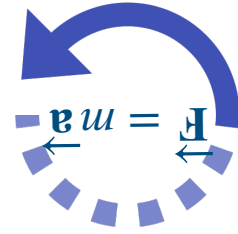
$$x = \begin{bmatrix} || \vec{F}_{1x} || \\ || \vec{F}_{1y} || \\ || \vec{T}_1 || \\ \vdots \\ || \vec{F}_{nx} || \\ || \vec{F}_{ny} || \\ || \vec{T}_n || \end{bmatrix} \begin{bmatrix} 0 \\ 0 \\ 0 \\ \vdots \\ 0 \\ 0 \\ 0 \end{bmatrix} = \begin{bmatrix} \sum \vec{F}_{x1} - m_1 a_{1x} \\ \sum \vec{F}_{y1} - m_1 a_{1y} \\ \sum \vec{T}_1 - I_1 \alpha_1 \\ \vdots \\ \sum \vec{F}_{xn} - m_n a_{nx} \\ \sum \vec{F}_{yn} - m_n a_{ny} \\ \sum \vec{T}_n - I_n \alpha_n \end{bmatrix} = A \cdot x - b$$

x is the vector of intersegmental force and joint torque quantities defined for every joint using

b is the vector of constant mass and inertial properties, and measured accelerations for every segment, and A is the matrix of all coefficients for the equations including every segment and joint.



HAB718 Spor Biyomekaniğinde Hareket Analizi



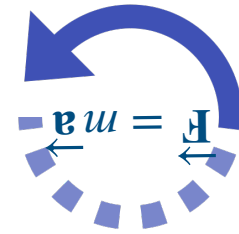
Inverse Dynamics

$$\begin{bmatrix} 0 \\ 0 \\ 0 \\ \vdots \\ 0 \\ 0 \\ 0 \end{bmatrix} = \begin{bmatrix} \sum \vec{F}_{x1} - m_1 a_{1x} \\ \sum \vec{F}_{y1} - m_1 a_{1y} \\ \sum \vec{T}_1 - I_1 \alpha_1 \\ \vdots \\ \sum \vec{F}_{xn} - m_n a_{nx} \\ \sum \vec{F}_{yn} - m_n a_{ny} \\ \sum \vec{T}_n - I_n \alpha_n \end{bmatrix} = A \cdot x - b$$

This equation has no exact solution since A is longer than x , but the least squares solution can be found by the optimization.

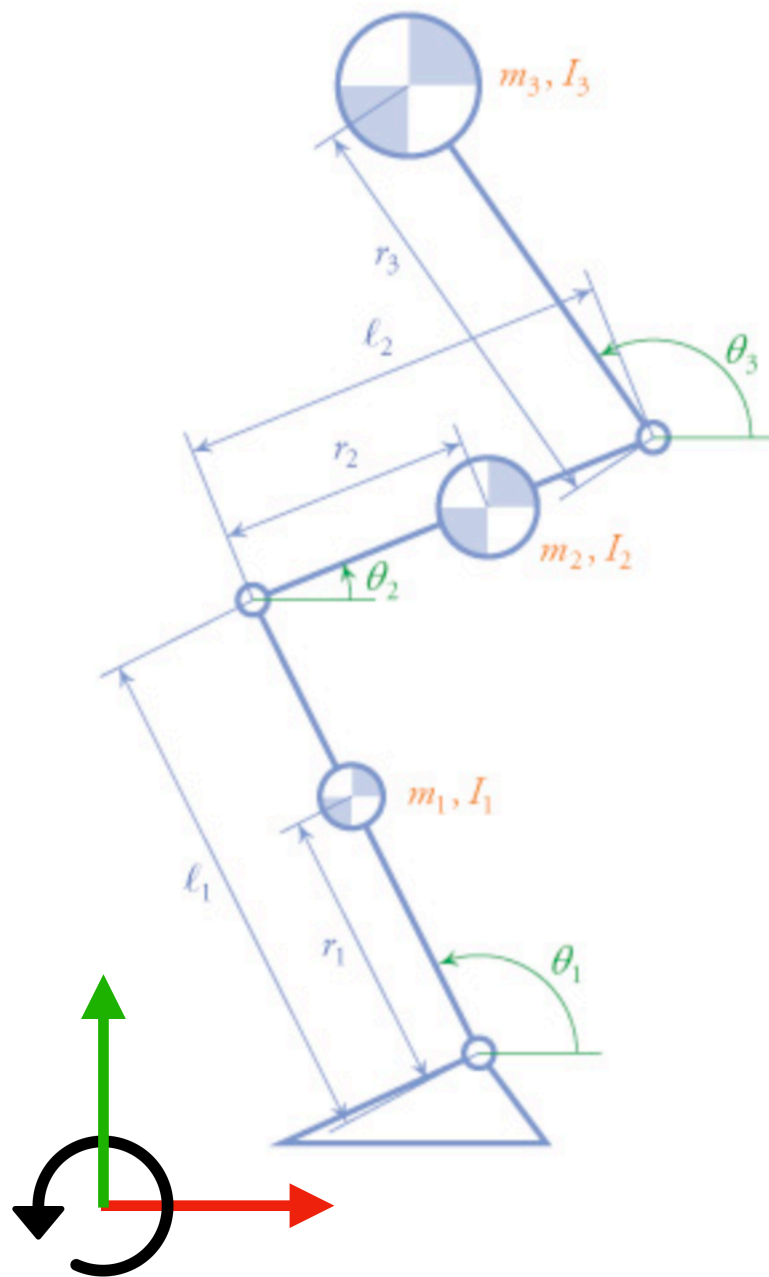
$$x = \operatorname{argmin}_x (|A \cdot x - b|^2) = (A^T \cdot A)^{-1} \cdot A^T \cdot b$$

HAB718 Spor Biyomekaniğinde Hareket Analizi



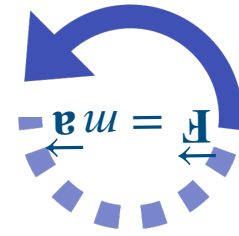
Inverse Dynamics

Inverse dynamics **with** ground reaction forces



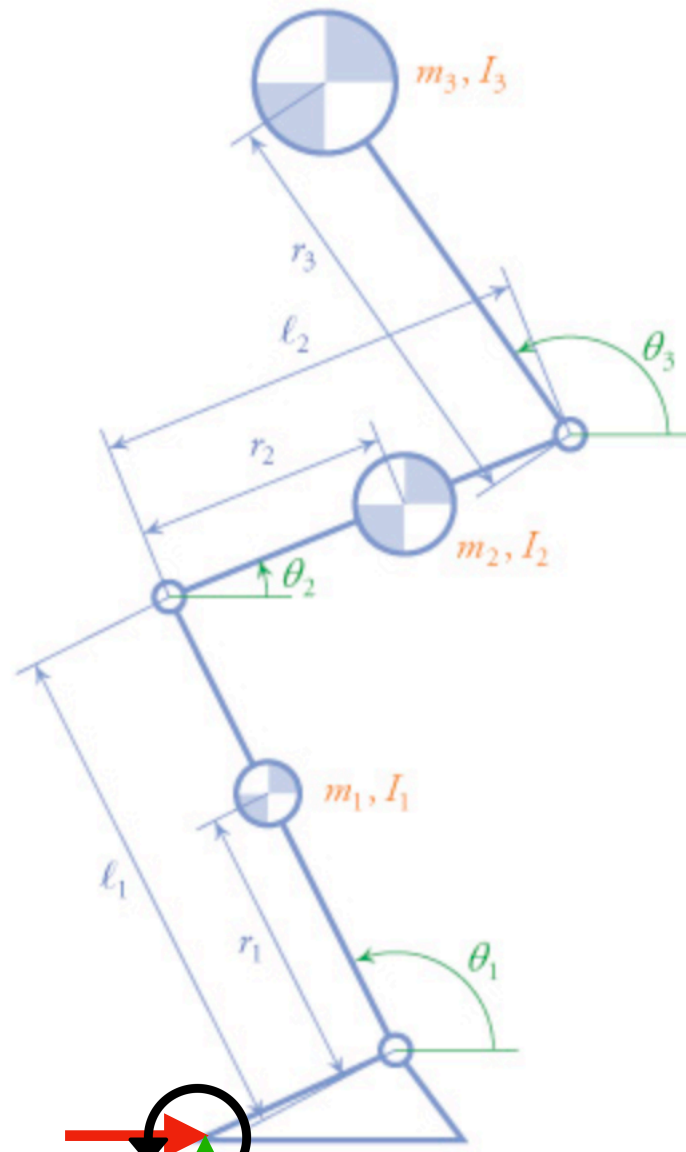
1. Create free-body diagram
 - Reaction forces & moments
 - Distance forces & moments
2. Form motion quantities (kinematics)
 - Positions (x, y, θ)
 - Velocities ($\dot{x}, \dot{y}, \dot{\theta}$)
 - Accelerations ($\ddot{x}, \ddot{y}, \ddot{\theta}$)
3. Apply Newton's 2nd law (kinetics)
 - Forces ($\sum F_x = m\ddot{x}$) ($\sum F_y = m\ddot{y}$)
 - Moments ($\sum M = I\ddot{\theta}$)

HAB718 Spor Biyomekaniğinde Hareket Analizi

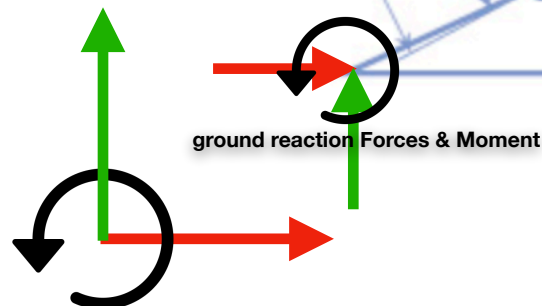


Inverse Dynamics

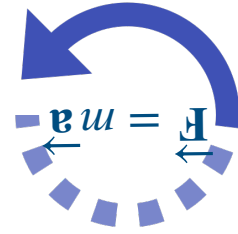
Inverse dynamics **with** ground reaction forces



- Planar, 3 degrees of freedom
- Position (orientation) in global coordinate system
- Segment length = l_i
- Distance to mass center length = r_i
- Moments of inertia about mass center
- Foot has no mass and remains on ground



HAB718 Spor Biyomekaniğinde Hareket Analizi



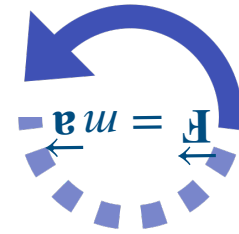
Inverse Dynamics

Inverse dynamics **with** ground reaction forces

$$A \cdot x = b$$

$$x = \begin{bmatrix} F_{x_1} \\ F_{x_2} \\ F_{y_1} \\ F_{y_2} \\ T_1 \\ T_2 \\ F_{x_3} \\ F_{y_3} \\ T_3 \end{bmatrix} \quad A = \begin{bmatrix} 1 & -1 & 0 & 0 & 0 & 0 & 0 & 0 & 0 \\ 0 & 0 & 1 & -1 & 0 & 0 & 0 & 0 & 0 \\ 1 & -1 & r_1 \sin \theta_1 & -r_1 \cos \theta_1 & (l_1 - r_1) \sin \theta_1 & (l_1 - r_1) \cos \theta_1 & 0 & 0 & 0 \\ 0 & 1 & 0 & 0 & 0 & 0 & -1 & 0 & 0 \\ 0 & 0 & 0 & 1 & 0 & 0 & 0 & -1 & 0 \\ 0 & r_2 \sin \theta_2 & 0 & -r_2 \cos \theta_2 & 0 & 1 & (l_2 - r_2) \sin \theta_2 & -(l_2 - r_2) \cos \theta_2 & -1 \end{bmatrix} \quad b = \begin{bmatrix} -m_1 r_1 (\sin \theta_1 \ddot{\theta}_1 + \cos \theta_1 \dot{\theta}_1^2) \\ m_1 (r_1 (\cos \theta_1 \ddot{\theta}_1 - \sin \theta_1 \dot{\theta}_1^2) + g) \\ I_1 \ddot{\theta}_1 \\ -m_2 (l_1 (\sin \theta_1 \ddot{\theta}_1 + \cos \theta_1 \dot{\theta}_1^2) + r_2 (\sin \theta_2 \ddot{\theta}_2 + \cos \theta_2 \dot{\theta}_2^2)) \\ m_2 (l_1 (\cos \theta_1 \ddot{\theta}_1 + \sin \theta_1 \dot{\theta}_1^2) + r_2 (\cos \theta_2 \ddot{\theta}_2 - \sin \theta_2 \dot{\theta}_2^2) + g) \\ I_2 \ddot{\theta}_2 \end{bmatrix}$$

HAB718 Spor Biyomekaniğinde Hareket Analizi

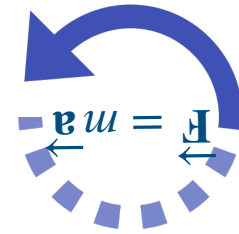


Inverse Dynamics

Inverse dynamics **with** ground reaction forces

$$x = \begin{bmatrix} \textcircled{F_{x_1}} \\ F_{x_2} \\ \textcircled{F_{y_1}} \\ F_{y_2} \\ \textcircled{T_1} \\ T_2 \\ F_{x_3} \\ F_{y_3} \\ T_3 \end{bmatrix} \begin{matrix} 1 \\ 2 \\ 3 \\ 4 \\ 5 \\ 6 \end{matrix} \quad b = \begin{bmatrix} -m_1 r_1 (\sin \theta_1 \ddot{\theta}_1 + \cos \theta_1 \dot{\theta}_1^2) \\ m_1 (r_1 (\cos \theta_1 \ddot{\theta}_1 - \sin \theta_1 \dot{\theta}_1^2) + g) \\ I_1 \ddot{\theta}_1 \\ -m_2 (l_1 (\sin \theta_1 \ddot{\theta}_1 + \cos \theta_1 \dot{\theta}_1^2) + r_2 (\sin \theta_2 \ddot{\theta}_2 + \cos \theta_2 \dot{\theta}_2^2)) \\ m_2 (l_1 (\cos \theta_1 \ddot{\theta}_1 + \sin \theta_1 \dot{\theta}_1^2) + r_2 (\cos \theta_2 \ddot{\theta}_2 - \sin \theta_2 \dot{\theta}_2^2) + g) \\ I_2 \ddot{\theta}_2 \end{bmatrix}$$

HAB718 Spor Biyomekaniğinde Hareket Analizi

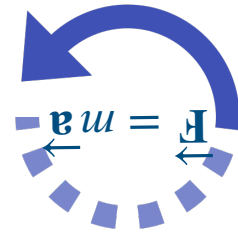


Inverse Dynamics

Inverse dynamics **with** ground reaction forces

$$A = \begin{bmatrix} 1 & -1 & 0 & 0 & 0 & 0 & 0 & 0 & 0 \\ 0 & 0 & 1 & -1 & 0 & 0 & 0 & 0 & 0 \\ 1 & -1 & r_1 \sin \theta_1 & -r_1 \cos \theta_1 & (l_1 - r_1) \sin \theta_1 & (l_1 - r_1) \cos \theta_1 & 0 & 0 & 0 \\ 0 & 1 & 0 & 0 & 0 & 0 & -1 & 0 & 0 \\ 0 & 0 & 0 & 1 & 0 & 0 & 0 & -1 & 0 \\ 0 & r_2 \sin \theta_2 & 0 & -r_2 \cos \theta_2 & 0 & 1 & (l_2 - r_2) \sin \theta_2 & -(l_2 - r_2) \cos \theta_2 & -1 \end{bmatrix}$$

HAB718 Spor Biyomekaniğinde Hareket Analizi

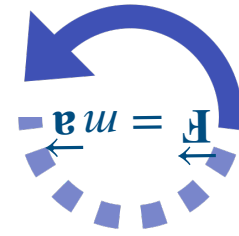


Inverse Dynamics

Inverse dynamics **without** ground reaction forces

$$x = \begin{bmatrix} F_{x_1} \\ F_{x_2} \\ F_{y_1} \\ F_{y_2} \\ T_1 \\ T_2 \\ F_{x_3} \\ F_{y_3} \\ T_3 \end{bmatrix} \quad b = \begin{bmatrix} -m_1 r_1 (\sin \theta_1 \ddot{\theta}_1 + \cos \theta_1 \dot{\theta}_1^2) \\ m_1 (r_1 (\cos \theta_1 \ddot{\theta}_1 - \sin \theta_1 \dot{\theta}_1^2) + g) \\ I_1 \ddot{\theta}_1 \\ -m_2 (l_1 (\sin \theta_1 \ddot{\theta}_1 + \cos \theta_1 \dot{\theta}_1^2) + r_2 (\sin \theta_2 \ddot{\theta}_2 + \cos \theta_2 \dot{\theta}_2^2)) \\ m_2 (l_1 (\cos \theta_1 \ddot{\theta}_1 + \sin \theta_1 \dot{\theta}_1^2) + r_2 (\cos \theta_2 \ddot{\theta}_2 - \sin \theta_2 \dot{\theta}_2^2)) \\ I_2 \ddot{\theta}_2 \\ -m_3 (l_1 (\sin \theta_1 \ddot{\theta}_1 + \cos \theta_1 \dot{\theta}_1^2) + l_2 (\sin \theta_2 \ddot{\theta}_2 + \cos \theta_2 \dot{\theta}_2^2) + r_3 (\sin \theta_3 \ddot{\theta}_3 + \cos \theta_3 \dot{\theta}_3^2)) \\ m_3 (l_1 (\cos \theta_1 \ddot{\theta}_1 - \sin \theta_1 \dot{\theta}_1^2) + l_2 (\cos \theta_2 \ddot{\theta}_2 - \sin \theta_2 \dot{\theta}_2^2) + r_3 (\cos \theta_3 \ddot{\theta}_3 - \sin \theta_3 \dot{\theta}_3^2) + g) \\ I_3 \ddot{\theta}_3 \end{bmatrix}$$

HAB718 Spor Biyomekaniğinde Hareket Analizi



Inverse Dynamics

Inverse dynamics **without** ground reaction forces

$$A = \begin{bmatrix} 1 & -1 & 0 & 0 & 0 & 0 & 0 & 0 & 0 \\ 0 & 0 & 1 & -1 & 0 & 0 & 0 & 0 & 0 \\ 1 & -1 & r_1 \sin \theta_1 & -r_1 \cos \theta_1 & (l_1 - r_1) \sin \theta_1 & (l_1 - r_1) \cos \theta_1 & 0 & 0 & 0 \\ 0 & 1 & 0 & 0 & 0 & 0 & -1 & 0 & 0 \\ 0 & 0 & 0 & 1 & 0 & 0 & 0 & -1 & 0 \\ 0 & r_2 \sin \theta_2 & 0 & -r_2 \cos \theta_2 & 0 & 1 & (l_2 - r_2) \sin \theta_2 & -(l_2 - r_2) \cos \theta_2 & -1 \\ 0 & 0 & 0 & 0 & 0 & 0 & 1 & 0 & 0 \\ 0 & 0 & 0 & 0 & 0 & 0 & 0 & 1 & 0 \\ 0 & 0 & 0 & 0 & 0 & 0 & r_3 \sin \theta_3 & -r_3 \cos \theta_3 & 1 \end{bmatrix}$$